



CHORUS

This is the accepted manuscript made available via CHORUS. The article has been published as:

BPS spectrum of supersymmetric CP(N-1) theory with $Z_{\{N\}}$ twisted masses

Pavel A. Bolokhov, Mikhail Shifman, and Alexei Yung

Phys. Rev. D **84**, 085004 — Published 5 October 2011

DOI: [10.1103/PhysRevD.84.085004](https://doi.org/10.1103/PhysRevD.84.085004)

BPS Spectrum of Supersymmetric $CP(N - 1)$ Theory with \mathcal{Z}_N Twisted Masses

Pavel A. Bolokhov^{a,b}, Mikhail Shifman^a and Alexei Yung^{a,c}

^a*William I. Fine Theoretical Physics Institute, University of Minnesota, Minneapolis, MN
55455, USA*

^b*Theoretical Physics Department, St.Petersburg State University, Ulyanovskaya 1,
Peterhof, St.Petersburg, 198504, Russia*

^c*Petersburg Nuclear Physics Institute, Gatchina, St. Petersburg 188300, Russia*

Abstract

We revisit the BPS spectrum of the supersymmetric $CP(N - 1)$ two-dimensional model with \mathcal{Z}_N -symmetric twisted masses m_l ($l = 0, 1, \dots, N - 1$). A related issue we address is that of the curves of marginal stability (CMS) in this theory. Previous analyses were incomplete. We close the gap by exploiting a number of consistency conditions. In particular, we amend the Dorey formula for the BPS spectrum. Our analysis is based on the exact Veneziano–Yankielowicz-type superpotential and on the strong-coupling spectrum of the theory found from the mirror representation at small masses, $|m_l| \ll \Lambda$. We show that at weak coupling the spectrum, with necessity, must include $N - 1$ BPS towers of states, instead of just one, as was thought before. Only one of the towers is seen in the quasiclassical limit. We find the corresponding CMS for these towers, and argue that in the large- N limit they become circles, filling out a band on the plane of a single mass parameter of the model at hand. Inside the CMS, $N - 1$ towers collapse into N stable states.

1 Introduction

Two-dimensional $\mathcal{N} = (2, 2)$ $\text{CP}(N - 1)$ model with twisted masses exhibits a remarkable similarity to certain four-dimensional gauge theories. The underlying reason was revealed in [1, 2] where the supersymmetric $\text{CP}(N - 1)$ model was demonstrated to emerge as a low-energy world-sheet theory on the non-Abelian strings, see [3, 4, 1, 2]. The coincidence between the BPS spectrum of the $\text{CP}(N - 1)$ model and that of $\mathcal{N} = 2$ SQCD in a quark vacuum observed in [5] received a natural explanation. Namely, these two spectra, in fact, describe the same states but from two different perspectives: viewed from the bulk and from the world sheet.

Superalgebra in the $\text{CP}(N - 1)$ model is centrally extended, with the central charge containing a topological term and $(N - 1)$ Noether charges. The former includes a canonical contribution and an anomalous one, which is especially obvious in the limit of the vanishing twisted masses (e.g. [6]). The contributions of the Noether charges are proportional to the twisted masses.

The masses of the BPS-saturated states reduce to the corresponding central charges. However, not every state is realized in the theory. The BPS spectrum depends on the value of the twisted masses m_l ($l = 0, 1, \dots, N - 1$). If $|m_l| \gg \Lambda$, we are at weak coupling. In this regime the BPS spectrum contains states characterized by the topological charge $T = \pm 1$, with infinite towers of heavier states with nonvanishing $\text{U}(1)$ charges built on them. Not all states possible algebraically are dynamically realized as stable states in the spectrum. If $|m_l| \ll \Lambda$, we are at strong coupling. The BPS spectrum of elementary kinks shrinks down to N stable states.

A general and detailed discussion of the BPS mass spectrum in the $\text{CP}(N - 1)$ model with the twisted masses was undertaken in [7, 5] on the basis of the Veneziano–Yankielowicz-type¹ superpotential [8] augmented by the twisted mass terms [7], in conjunction with a quasiclassical analysis. A concrete implementation of the spectrum of the dynamically realized BPS states on both sides of the CMS (as well as the CMS itself) in the $\text{CP}(1)$ model was constructed in [6]. For $N > 2$ in the case of \mathcal{Z}_N -symmetric twisted masses the issue of the BPS spectrum and the CMS separating the strong and weak-coupling domains was addressed in [9] and, later, in [10]. The latter two studies were based on the Dorey formula which, as we will show in this paper, is by far incomplete. The advantage of the \mathcal{Z}_N -symmetric twisted masses compared to a generic set is rather obvious. Generally speaking, we have $N - 1$ twisted masses implying the parameter space of the complex dimension $N - 1$ (in this case it is more appropriate to speak of the decay walls rather than curves). Starting from $N = 3$ and higher, with generic masses, explicit analytic determination of the BPS spectra and

¹The Veneziano–Yankielowicz superpotential in the $\text{CP}(N - 1)$ models with no twisted masses was originally derived, in terms of twisted superfields, in [16, 17, 14].

CMS, even if possible, ceases to be instructive. On the other hand, with the \mathcal{Z}_N -symmetric twisted masses, the model depends on a single complex mass parameter, everything becomes simple, and the would-be decay walls reduce to a set of CMS in the complex plane of m_0 , a single complex parameter defining all twisted masses. On the physical side the advantage of the \mathcal{Z}_N -symmetric choice is also obvious: with this choice the twisted masses preserve the \mathcal{Z}_N subgroup of the \mathcal{Z}_{2N} symmetry of the massless model, which is a remnant of the axial R symmetry. Physics of the transition from weak to strong coupling becomes transparent.

Our goal here is to work out a complete solution of this question. Technically the problem is due to the fact that the Veneziano–Yankielowicz (VY) superpotential is a multivalued function and, in calculating the BPS spectrum, one needs to carefully analyze its branches in order to select those which can be dynamically realized. We add two crucial ingredients missing in [5]. First, in the small- $|m_l|$ limit the BPS spectrum is known [11] from the Hori–Vafa representation [12]. In other words, the mirror symmetry is instrumental in finding the BPS spectrum. At strong coupling only $N - 1$ stable states exist. These are the states that become massless at the Argyres–Douglas points [13], at which vacua collide. In our case, the \mathcal{Z}_N -symmetric masses, all vacua collide simultaneously. The vanishing mass requirement at this point, in conjunction with small mass formula, enables us to resolve the ambiguity in the VY superpotential and determine the spectrum of masses of stable BPS states both outside and inside the CMS in its entirety. We arrive at the conclusion that the spectrum found in [5] and consisting of a single BPS tower (for kinks interpolating between a given pair of vacua) is not capable of satisfying all the above requirements. We argue that the theory must instead have $N - 1$ towers, each of which is described by its own $U(1)$ quantum number. We find this natural in view of the fact that the global $SU(N)$ symmetry is broken down to $U(1)^{N-1}$ by the twisted masses. For each of these $U(1)$'s there is a tower of states arising from quantization. Only one tower is distinctly seen in the quasiclassical treatment, however, and that makes it special. That is the tower described in [5]. All others are not resolved: in the quasiclassical limit which corresponds to large $|m_l|$ and large $U(1)$ quantum numbers all $N - 1$ towers fuse with each other.

With the BPS spectrum in hands we pass to the second stage: determination of the curves of marginal stability in the same $CP(N - 1)$ model with \mathcal{Z}_N -symmetric twisted masses. For each of the BPS towers there must be a curve on which the relevant states decay. Altogether, we deal here with $N - 1$ curves of marginal stability. We find that the curve corresponding to the special “quasiclassical” tower always passes through the Argyres–Douglas point. For this reason we will call it *primary*. The primary curve is the innermost curve on the complex plane of m_0 , inside which only strong coupling states are stable. Other, secondary, curves are larger in size and are (typically) near-perfect circles. When passing from the weak coupling domain into the strong coupling one, the towers of states decay on these curves, one by one. Finally, we consider the large- N limit of the theory and show that in this limit all CMS tend

to round circles, with radii in the interval

$$1 \leq |m|/\Lambda \leq e^2, \quad (e = 2.71828\dots) \quad (1.1)$$

in units of the low-energy scale Λ . In the limit of very large N the curves of marginal stability completely fill this interval, forming a round band.

Organization of the paper is as follows. In Sec. 2 we review the gauged formulation of the model and present the VY superpotential with the twisted mass included. In Sec. 3 we consider predictions for the BPS spectrum at small $|m_0|$ following from the mirror symmetry. Section 4 is devoted to the Argyres–Douglas (AD) point. In Sec. 5 we obtain the complete BPS spectrum both at strong and weak coupling based on the VY superpotential and the conditions outlined above. Construction of $N - 1$ curves of marginal stability is the subject of Sec. 6. Section 8 presents a summary of our results.

2 Exact Superpotential

In the gauged formulation, the bosonic part of the Lagrangian of the $\mathcal{N} = (2, 2)$ supersymmetric $\text{CP}(N - 1)$ theory can be obtained from four-dimensional SQED with an N -plet chiral superfield, by a dimensional reduction to two dimensions [14, 7],

$$\begin{aligned} \mathcal{L} = & \frac{1}{e_0^2} \left(\frac{1}{4} F_{\mu\nu}^2 + |\partial_\mu \sigma|^2 + \frac{1}{2} D^2 \right) + |\nabla_\mu n^i|^2 \\ & + i D (|n_i|^2 - 2\beta) + 2 \sum_i \left| \sigma - \frac{m_i}{\sqrt{2}} \right|^2 |n^i|^2. \end{aligned} \quad (2.1)$$

in the strong-coupling limit $e_0 \rightarrow \infty$. Here e_0 is the gauge coupling while m_i are the complex twisted mass parameters which can be introduced [15] via a background vector field in four dimensions. Moreover, 2β can be viewed as a coupling of the corresponding sigma model (sometimes $r \equiv 2\beta$ is used).

We should mention that physically the mass parameters are not given by the masses m_l themselves, but, rather, by their differences $m_l - m_k$ (or by $m_l - m$, where m is the average mass). This is clear from Eq. (2.1) as one can shift all masses by any value via a redefinition of σ . Thus, one can always impose the condition

$$\sum_{l=0}^{N-1} m_l = 0. \quad (2.2)$$

With arbitrary choice of masses we break the global $\text{SU}(N)$ invariance of the model down to $\text{U}(1)^{N-1}$. We are interested in a special case when the masses are assumed to

preserve a discrete \mathcal{Z}_N subgroup of the anomalous $U(1)_R$ symmetry. To this end they must sit equidistantly on a circle,

$$m_l = m_0 \cdot e^{2\pi i l/N}, \quad l = 0, 1, \dots, N-1, \quad (2.3)$$

with a single complex parameter m_0 defining all masses. The condition (2.2) is automatically met. We will see that in the $CP(N-1)$ model, the physical dependence of the theory is, in fact, on m_0^N .

The theory (2.1) classically has N vacua, which can be seen as solutions with all n_i but one set to zero,

$$\begin{aligned} n_i &= (0, \dots, 1, \dots, 0), & k &= 0, \dots, N-1, \\ \sigma &= m_k. \end{aligned} \quad (2.4)$$

Note that we choose to number both the masses and the vacua from 0 to $N-1$.

The chiral sector of this theory is described by an exact superpotential of the Veneziano–Yankielowicz type [8]. For a theory with twisted masses the Veneziano–Yankielowicz superpotential was derived in [16, 17, 14, 7], and is obtained by integrating out the n^l fields in Eq. (2.1),

$$\mathcal{W}_{\text{eff}}(\hat{\sigma}) = -i\tau\hat{\sigma} + \frac{1}{2\pi} \sum_j (\hat{\sigma} - m_j) \left\{ \ln \frac{\hat{\sigma} - m_j}{\mu} - 1 \right\}. \quad (2.5)$$

The hat over $\hat{\sigma}$ indicates that it is actually a (twisted) superfield. In passing from (2.1) to (2.5) we rescaled σ ,

$$\sigma \rightarrow \frac{\sigma}{\sqrt{2}}. \quad (2.6)$$

In Eq. (2.5) τ is the complexified coupling,

$$\tau = ir + \frac{\theta}{2\pi}, \quad \text{with } r \equiv 2\beta. \quad (2.7)$$

The ultraviolet cut-off scale μ can be traded for the dynamical scale Λ ,²

$$\mu = \Lambda e^{2\pi r/N}, \quad (2.8)$$

where r in the exponent on the right-hand side corresponds to the same normalization point μ . Then, the first term on the right-hand side of (2.5) disappears while μ in the argument of logarithms is replaced by Λ . The $CP(N-1)$ model is asymptotically free.

²Without a loss of generality one can always assume Λ to be real and positive. We will stick to this convention. A possible phase of Λ is absorbed in m_0 .

Now, Witten's formula [14] for the positions of vacua is

$$\prod_{l=0}^{N-1} (\sigma - m_l) = \Lambda^N. \quad (2.9)$$

This is the equation for critical points of $\mathcal{W}_{\text{eff}}(\sigma)$. With the set of masses (2.3) Eq. (2.9) implies that the vacua of this theory are at

$$\sigma_p = \sqrt[N]{\Lambda^N + m_0^N} \cdot e^{2\pi i p/N}, \quad p = 0, \dots, N-1. \quad (2.10)$$

Altogether, we have N vacua, in full accord with Witten's index.

If $|m_0|$ is taken to be large, then it dominates over Λ in (2.10), and the vacua take their classical values (2.4),

$$\sigma_p \approx m_p, \quad p = 0, \dots, N-1. \quad (2.11)$$

In future, for determination of the BPS spectrum, we will need the values of the superpotential in the vacuum. It is not difficult to get

$$\mathcal{W}_{\text{eff}}(\sigma_p) = -\frac{1}{2\pi} \left\{ N \sigma_p + \sum_j m_j \ln \frac{\sigma_p - m_j}{\Lambda} \right\}. \quad (2.12)$$

Various choices of the branches of the logarithms above correspond to distinct values of the Noether $U(1)$ charges.

In deriving expression (2.12) we used the Witten's relation (2.9). With our normalization, the general formula for the mass of an *elementary* BPS state reduces to the difference of superpotentials in two neighboring vacua,

$$m_{\text{BPS}} = \left| \mathcal{W}_{\text{eff}}(\sigma_{p+1}) - \mathcal{W}_{\text{eff}}(\sigma_p) \right|. \quad (2.13)$$

Note that the elementary kinks are obtained if one interpolates between the neighboring vacua. The result is the same independently of which pair of neighbors we pick up. This is due to the \mathcal{Z}_N symmetry of the model.

With the \mathcal{Z}_N -symmetric masses (2.3), the theory at quantum level retains the \mathcal{Z}_N symmetry, which the masses do not break. This symmetry manifests itself in the invariance of the spectrum to the choice of vacua in (2.13). From now on we will choose the vacua σ_0 and σ_1 as representatives and focus on the masses of kinks interpolating between the two,

$$m_{\text{BPS}} = \left| \mathcal{W}_{\text{eff}}(\sigma_1) - \mathcal{W}_{\text{eff}}(\sigma_0) \right| \quad (2.14)$$

(in bulky expressions, we will omit the absolute value sign, keeping it in mind; certainly, m_{BPS} is always a positive quantity).

In the quasiclassical limit $|\Delta m| \gg \Lambda$ the leading contribution to the mass is given by the dominant logarithm in expression (2.14),

$$\mathcal{W}_{\text{eff}}(\sigma_1) - \mathcal{W}_{\text{eff}}(\sigma_0) \sim \frac{N}{2\pi} \Delta m \cdot \ln \frac{|m_0|}{\Lambda} = r \cdot \Delta m, \quad (2.15)$$

where $\Delta m = m_1 - m_0$.

It is well-known that the Veneziano–Yankielowicz potential, being a multi-branch function, is too ambiguous. The degree of ambiguity of expression (2.14) is determined by the logarithms in (2.12), and can be symbolized by a linear combination of the masses m_j with arbitrary integer coefficients

$$\langle \text{integer} \rangle_j \cdot m_j. \quad (2.16)$$

If all these multiplicities were physical, one would have a set of \mathcal{Z}^N states in the spectrum, which is certainly not what is expected. Selection rules need to be formulated in order to restrict the set of the BPS states that actually exist. We postpone the formulation of these rules until further, while for now do a simple mathematical trick which reduces the amount of ambiguity present in Eq. (2.14). Our goal is to turn (2.14) being a function of all masses and two vacua into a function of a single parameter m_0 .

Let us pull out a factor of $e^{2\pi i/N}$ from each term in $\mathcal{W}_{\text{eff}}(\sigma_1)$ which originally looks as,

$$\mathcal{W}_{\text{eff}}(\sigma_1) = -\frac{1}{2\pi} \left\{ N \sigma_1 + \sum_j m_j \ln \frac{\sigma_1 - m_j}{\Lambda} \right\}. \quad (2.17)$$

Both terms in Eq. (2.17) do contain this factor. This move turns σ_1 into σ_0 , while shifts the numeration of masses in the sum. To keep the numeration of masses in the sum consonant with the logarithms, we also pull out $e^{2\pi i/N}$ from the argument of the logarithm. This constant addition vanishes when summed with $\sum m_j$, while σ_1 inside the logarithm again turns into σ_0 . Effectively one arrives at

$$\mathcal{W}_{\text{eff}}(\sigma_1) \stackrel{?}{=} e^{2\pi i/N} \mathcal{W}_{\text{eff}}(\sigma_0). \quad (2.18)$$

The question mark in (2.18) reminds us that this is not quite the whole story. We were not very careful with the phases of the logarithms, and could have easily missed (and actually did) some $2\pi i$. This owes to the fact that $\ln ab = \ln a + \ln b$ only modulo $2\pi i$. But such an omission can just as well be merged into the general ambiguity (2.16) of the expression (2.14). We can fuse this ambiguity into a single linear combination $i \vec{N} \cdot \vec{m}$, where \vec{N} is an arbitrary constant integer vector, $\vec{N} = (n_0, \dots, n_{N-1})$ with integer n_i and $\vec{m} = (m_0, \dots, m_{N-1})$. Now we rewrite (2.14) as,

$$m_{\text{BPS}} = U_0(m_0) + i \vec{N} \cdot \vec{m}, \quad (2.19)$$

with an explicit function

$$U_0(m_0) = -\frac{1}{2\pi} \left(e^{2\pi i/N} - 1 \right) \left\{ N \sqrt[N]{m_0^N + \Lambda^N} + \sum_j m_j \ln \frac{\sqrt[N]{m_0^N + \Lambda^N} - m_j}{\Lambda} \right\}. \quad (2.20)$$

The branch of U_0 is fixed as follows: if x is a real positive number, (i) $\sqrt[N]{x}$ is a real positive number; (ii) $\ln x$ is a real number. Here m_j is meant to be a function of m_0 as well, via (2.3).

The important statements are,

- In Eq. (2.19) all ambiguities related to the logarithms are referred to \vec{N} ;
- Now $U_0(m_0)$ is a fixed single-valued function of the complex parameter m_0 in a certain region of the complex plane.
- Vector \vec{N} in Eq. (2.19) has a direct relation to the spectrum.

Let us briefly comment on what is meant. The BPS spectrum exists everywhere on the complex plane of m_0 , and both expressions (2.14) and (2.19) must in principle describe it. But for that, they need to be made unambiguous at least in some region of the complex plane of m_0 . We claim that function $U_0(m_0)$ is single-valued in a domain of the complex plane wide enough to unambiguously determine the spectrum. The latter will be described in terms of the vector \vec{N} . Exactly how wide the domain of the parameter m_0 needs to be will be discussed in Section 5. It will also become clear why Eq. (2.19) is more directly related to the determination of the spectrum than Eq. (2.14).

In this way we will arrive at our master formula. We will be able to determine such an expression for the spectrum which will be consistent both at large and small $|m|$. In particular, we will find that the prescription obtained in [5],

$$\vec{N} = (-n, n, 0, \dots, 0), \quad n \in \mathcal{Z}, \quad (2.21)$$

is valid only approximately, in the quasiclassical limit, which corresponds to large $|m|$ and large excitation number n . The result (2.21) was derived by quasiclassical quantization of the time rotation of kinks in the U(1) factors of the global group, and, therefore, must still be valid as an *asymptotics*. Below we argue, however, that the description (2.21) is incomplete.

3 Mirror Treatment

Now we gradually pass to the discussion of what is known about the strong coupling regime. There are N BPS kinks. They can be seen in the mirror representation [12, 18],

$$\mathcal{W}_{\text{mirror}}^{\text{CP}(N-1)} = -\frac{\Lambda}{2\pi} \left\{ \sum_j X_j + \sum_j \frac{m_j}{\Lambda} \ln X_j \right\}, \quad (3.1)$$

with

$$\prod_j X_j = 1. \quad (3.2)$$

As was shown in [11], one can determine the masses of all N kinks near the origin, $|m_j| \ll \Lambda$,

$$m_{\text{BPS}} \approx \left| \frac{N}{2\pi} \left(e^{2\pi i/N} - 1 \right) \Lambda - i(m_j - m) \right|, \quad (3.3)$$

where m is the average mass, vanishing in the \mathcal{Z}_N case. So, to the linear order in the mass parameter, one has N kinks with the masses given by a large Λ term, and the splittings determined by m_j themselves,

$$m_{\text{BPS}} \approx \left| \frac{N}{2\pi} \left(e^{2\pi i/N} - 1 \right) \Lambda - i m_j \right|, \quad j = 0, \dots, N-1. \quad (3.4)$$

4 Argyres–Douglas Point

If all masses m_j sit on a circle the corresponding vacua will also be forced to sit on a circle, see (2.10). Therefore, only simultaneous collisions of all N vacua σ_p take place in the theory at hand. The Argyres–Douglas points [13] correspond to

$$\sigma_p = 0. \quad (4.1)$$

This occurs whenever $m_0^N = -\Lambda^N$, or, in the m_0 plane,

$$m_0^{\text{AD}} = \Lambda e^{i\pi/N} \cdot e^{2\pi i l/N}, \quad l = 0, \dots, N-1. \quad (4.2)$$

Of these, the most convenient for us will be the two AD points closest to the real positive axis,

$$m_0^{\text{AD(I)}} = \Lambda e^{i\pi/N} \quad \text{and} \quad m_0^{\text{AD(II)}} = \Lambda e^{-i\pi/N}. \quad (4.3)$$

The crucial observation about the AD point is that one of the N soliton states (3.4) becomes massless at that location in the complex m_0 plane. Briefly, if all the vacua merge at the AD point, then Eq. (2.14) tells one that one of the kinks becomes massless

$$m_{\text{BPS}} = \mathcal{W}_{\text{eff}}(\sigma_1) - \mathcal{W}_{\text{eff}}(\sigma_0) = 0. \quad (4.4)$$

Here we quote this as a qualitative statement and render it more precise in Section 5. For now it is almost trivial to note that, although both superpotential functions here are multivalued, there exists a *certain* branch on which the above difference vanishes.

5 BPS Spectrum

We now turn to the discussion of the BPS spectrum in detail, with an emphasis on the strong coupling domain. Surprisingly, the conclusions obtained in the strong coupling sector will allow us to make implications for the weak coupling sector as well. We first collect the results known and trustworthy about the CP(1) model [6], as the simplest and well-studied case, and then increase N .

5.1 CP(1) Spectrum

There are two kinks in the strong coupling sector with quantum numbers

$$(T, n) = (1, 0) \quad \text{and} \quad (T, n) = (1, 1).$$

Here T bears the conventional meaning of the topological charge, the constant that multiplies $\mathcal{W}_{\text{eff}}(\sigma_1) - \mathcal{W}_{\text{eff}}(\sigma_0)$, and $n \in \mathcal{Z}$ is the Noether charge, connected with the angle collective coordinate of the unbroken U(1).

The formula for the BPS mass in the CP(1) theory is well-known. We recover it from our master equations (2.19) and (2.20),

$$m_{\text{BPS}}^{\text{CP}(1)} = \frac{1}{\pi} \left(2 \sqrt{m_0^2 + \Lambda^2} - m_0 \ln \frac{\sqrt{m_0^2 + \Lambda^2} + m_0}{\sqrt{m_0^2 + \Lambda^2} - m_0} \right) + i \vec{N} \cdot \vec{m}. \quad (5.1)$$

The Argyres–Douglas points here are $m_0^{\text{AD}} = \pm i\Lambda$, and correspond to the vanishing square root. Let us trace how different states become massless at these AD points. Say, choose the branch of the logarithm such that at the point $m_0 = i\Lambda$ the logarithm equals $i\pi$. Then the kink $\vec{N} = (1, 0)$ becomes massless at this point. Let us move from the point $i\Lambda$ to $-i\Lambda$ along a large circle, see Fig 1a. It is easy to show that the argument of the logarithm in Eq. (5.1) will also follow a large circle, starting and terminating at -1 , see Fig 1b. However, this contour arrives to -1 from under the cut of the logarithm, and, therefore, the phase of the argument of the logarithm changes from $i\pi$ to $-i\pi$. As a result, the kink masses now shift compared to $m_0 = +i\Lambda$ point,

$$m_{\text{BPS}}^{\text{CP}(1)}(-i\Lambda) = i m_0 + i \vec{N} \cdot \vec{m}. \quad (5.2)$$

One observes, that it is a different kink which becomes massless now (it actually is the $(T, n) = (1, 1)$ kink, as we will see in a moment). It is not difficult to see that for this kink $\vec{N} = (0, 1)$.

Let us show that Eq. (5.1) is in one-to-one correspondence with the result from the mirror theory (3.4). At small m_0 , the argument of the logarithm in Eq. (5.1) just turns into 1, while

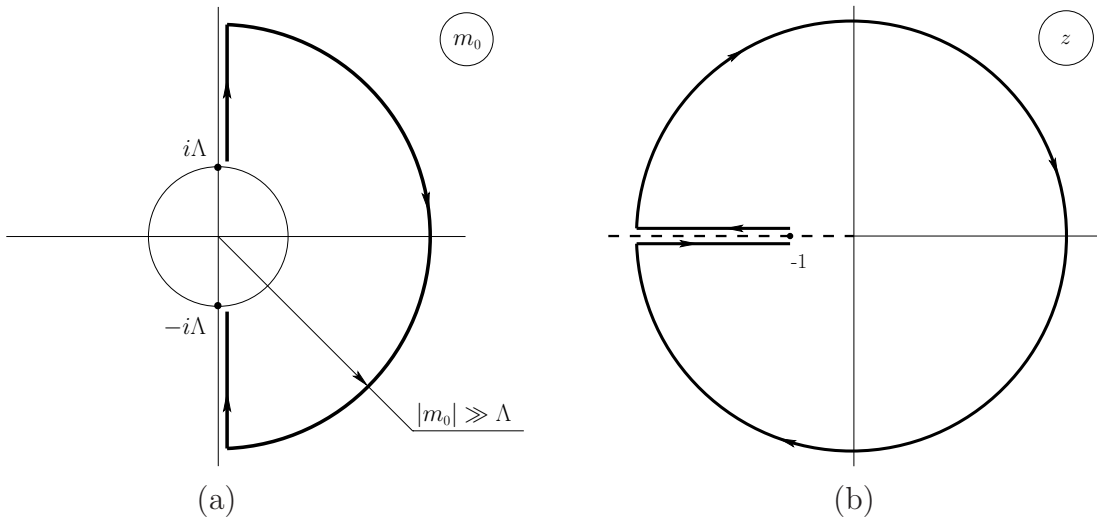


Figure 1: (a) The large-radius contour in the m_0 plane, starting at the AD point $i\Lambda$ and terminating at the point $-i\Lambda$. (b) The same contour shown in the plane of z — the argument of the logarithm in Eq. (5.1).

the first term in the bracket tends to Λ ,

$$m_{\text{BPS}}^{\text{CP}(1)} \rightarrow \frac{1}{\pi} 2\Lambda + i \vec{N} \cdot \vec{m}. \quad (5.3)$$

This does indeed agree with the spectrum (3.4), if we define the two states to be

$$\vec{N} = (1, 0) \quad \text{and} \quad \vec{N} = (0, 1). \quad (5.4)$$

These are the two states of the strong coupling regime. How does it happen that at weak coupling one has the whole tower of states while at strong coupling there are only two? Similar to what occurs in the Seiberg–Witten theory, the states of the weak coupling sector decay on the curves of marginal stability [19, 20, 21]. Only two states (5.4) survive when crossing into the strong coupling region, and those are precisely the states which become massless at the Argyres–Douglas points.

The kinks (5.4) therefore must be part of the weak coupling spectrum. We must be able to write a general formula for the latter, keeping in mind the quasiclassical asymptotic (2.21). Indeed, if one allows \vec{N} to be of the form

$$\vec{N} = (-n + 1, n), \quad n \in \mathcal{Z}, \quad (5.5)$$

then the two kinks (5.4) correspond to $n = 0$ and $n = 1$. On the other hand, at *large* n Eq. (5.5) does reproduce the quasiclassical tower (2.21). We stress that it is Eq. (5.5) that

describes the exact spectrum. The latter was obtained based on a meaningful and single-valued formula (2.19). In this illustrative example of CP(1), we stayed within one sheet of the logarithm.

We need to mention, that for CP(1) (and only for CP(1)) our results are not incompatible with those found in [5] and described by Eq. (2.21),

$$(-n, n), \quad n \in \mathcal{Z}. \quad (5.6)$$

The reason is that the extra unity found in (5.5) can be included into the logarithm in Eq. (5.1). That will alter the sign of the expression under the logarithm, after which Eq. (5.1) will match with the analogous expression quoted in [5] precisely. Already at CP(2) we will find that this coincidence is not valid.

To summarize, the spectrum for the CP(1) theory is given by equations (5.1) and (5.5), where n runs through all integer numbers in the weak coupling region, while it is restricted to $n = 0$ or $n = 1$ in the strong coupling domain.

5.2 General criteria

We can now formulate the *requirements* for the spectrum of BPS states in the overall region of the complex mass parameter m_0 :

- *Quasi-classical limit* — the spectrum at large m_0 and large excitation number n must reproduce the semiclassical result (2.15), (2.21):

$$m_{\text{BPS}} \simeq \frac{N}{2\pi} (m_1 - m_0) \cdot \ln \frac{|m_0|}{\Lambda} + i n \cdot (m_1 - m_0); \quad (5.7)$$

- *Argyres–Douglas point* — the only states that survive when crossing from weak coupling into the strong coupling region are those N states which become massless at the AD points;
- *Mirror spectrum* — the latter N kinks must reflect the spectrum given by mirror formula (3.4) in the small m_0 limit.

Having formulated the criteria for spectrum selection from the variety of branches of the logarithms of the Veneziano–Yankielowicz superpotential, we can now proceed to higher N . Of these, CP(2) will be the first nontrivial example.

5.3 Domain of m_0

At first we address the question of the relevant domain of variation for the parameter m_0 . Needless to say, both Eq. (2.14) and (2.19) are multivalued in the complex plane of m_0 . The

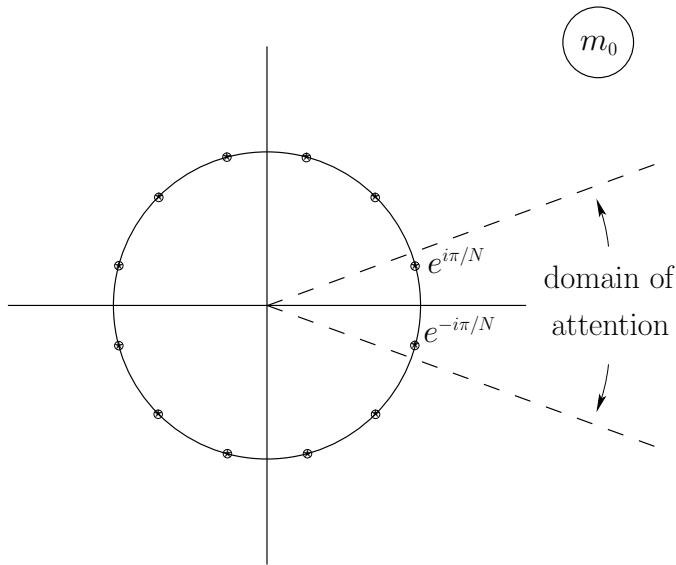


Figure 2: The domain of variation of m_0 free of branch cuts

analysis of the actual complex manifold of m_0 with all its branch cuts is a separate problem. We do not need such an extended analysis for our purposes, however. We can limit ourselves to the domain

$$-\pi < \text{Arg} (m_0^N) < \pi. \quad (5.8)$$

The exploitation of the criteria formulated in Sec. 5.2 relies on the possibility of using the formula (2.19) (i) in the neighborhood of the Argyres–Douglas point; (ii) in the neighborhood of $m_0 = 0$, and (iii) in the region of large $|m_0|$ — such that there are no discontinuities (*i.e.* branch cuts) between these regions.

The second goal is the calculation of the curves of marginal stability, which in principle does require one to move over the whole complex plane of m_0 . One can use the physical 2π periodicity in the θ angle to argue that the spectrum of the theory must be identical in the N sectors $\{ e^{2\pi i k/N} \dots e^{2\pi i(k+1)/N} \}$ of m_0 (although there might be a monodromy between the sectors). The spectrum and the curves of marginal stability will therefore repeat themselves in all these sectors, and thus it is enough to build them in a sector $2\pi/N$ wide in $\text{Arg} m_0$.

We choose the sector between the two Argyres–Douglas points

$$m_0^{\text{AD}} = \Lambda e^{i\pi/N} \quad \text{and} \quad m_0^{\text{AD}} = \Lambda e^{-i\pi/N}, \quad (5.9)$$

see Fig. 2. On the one hand the AD points are a useful reference, since the (smallest) curve of the marginal stability with necessity passes through the AD point (see Section 6). On the other hand, similar to what we did in $\text{CP}(1)$, we will be able to identify the states that

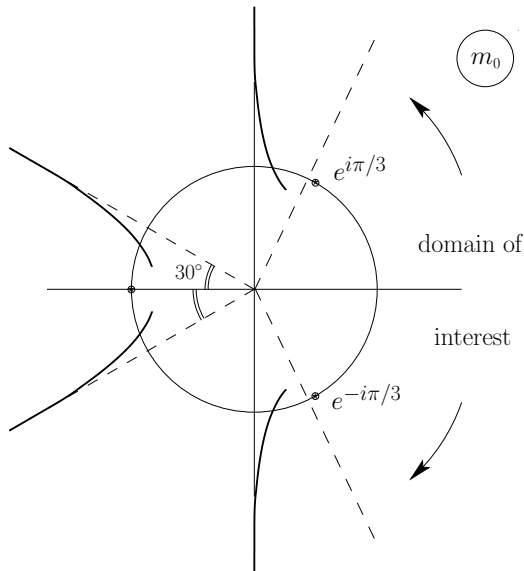


Figure 3: The Argyres–Douglas points in $\text{CP}(2)$ theory (in the units of Λ). Two points $e^{\pm i\pi/N}$ lie within our area of interest. The third one is separated from our area by branch cuts of the logarithms, shown with black solid lines.

become massless at the (at least these two) AD points. To this end it will be useful to be able to move from one AD point to another.

Third, and perhaps most important, our function (2.20) is *free* of the branch cuts in the region (5.9). This is, perhaps, the most drastic difference from the function in the right-hand side of Eq. (2.14) which does have branch cuts in this region.

One might want to move beyond the boundaries of the domain (5.9), for example, in order to approach other AD points. Although, as we argued, we do not need that for our purposes, we will partly be able to address the latter aspect.

5.4 Spectrum in $\text{CP}(2)$

The case of $\text{CP}(2)$ is sufficiently straightforward so that one can analyze function $U_0(m_0)$ in detail,

$$U_0(m_0) = -\frac{1}{2\pi} \left(e^{2\pi i/3} - 1 \right) \left\{ 3\sqrt[3]{m_0^3 + \Lambda^3} + \sum_j m_j \ln \frac{\sqrt[3]{m_0^3 + \Lambda^3} - m_j}{\Lambda} \right\}. \quad (5.10)$$

There are three Argyres–Douglas points in $\text{CP}(2)$, of which we will be interested in just two, see Fig. 3. The third one, $m_0^{\text{AD(III)}} = -1$ in the units of Λ , is separated by a pair of branch cuts of $U_0(m_0)$ from each of our primary AD points. The branch cuts start at infinity (*i.e.*

in the semiclassical regime) and continue into the strong coupling area, terminating inside the unit circle (it is to some degree a matter of convention where to terminate the branch cuts). Since we always prefer to move along circles of a large radius in order to stay away from the strong coupling area, these latter cuts prevent us from smoothly connecting to the third AD point. Nevertheless, we will still have our say about that point.

In between the AD points $m_0^{\text{AD(I)}} = e^{i\pi/3}$ and $m_0^{\text{AD(II)}} = e^{-i\pi/3}$ there are no branch cuts for (5.10), and one can smoothly commute between them. On the other hand, it can be shown that the right-hand side of Eq. (2.14) *does* have branch cuts in our area of attention, and therefore, although not impossible, when moving from one AD point to the other extra caution needs to be exercised.

The function $U_0(m_0)$ contains three logarithms, and it is easy to calculate its value at the AD points. At $m_0^{\text{AD(I)}} = e^{i\pi/3}$ it reduces to

$$U_0(e^{i\pi/3}) = -i m_0 = -i e^{i\pi/3}. \quad (5.11)$$

Therefore, a kink $\vec{N} = (1, 0, 0)$ becomes massless at this point. On the other hand, it is straightforward to calculate the BPS mass in the small m_0 limit — the whole function (5.10) only gives a zero-order contribution in the mass, the only linear term being given by $i\vec{N} \cdot \vec{m} = i m_0$,

$$m_{\text{BPS}} = -\frac{3}{2\pi} \left(e^{2\pi i/3} - 1 \right) \Lambda + i m_0. \quad (5.12)$$

This is precisely one of the kinks described by the mirror formula (3.4).

We can now smoothly slide from the AD point $e^{i\pi/3}$ to the one $e^{-i\pi/3}$, along a large radius contour (*i.e.* we first radially reach a circle of a large radius, and then sketch an arc extending clockwise to $\text{Arg } m_0 = -\pi/3$, after which, finally radially returning to the unit circle distance; see Fig. 4 where such a contour is shown for the case of general N). One can show by tracing the corresponding contours for $\sqrt[3]{m_0^3 + \Lambda^3} - m_j$ that neither of the logarithms of Eq. (5.10) steps over a branch cut. At the lower AD point, one has

$$U_0(e^{-i\pi/3}) = -i m_1 = -i e^{i\pi/3}, \quad (5.13)$$

with the same numerical value, the logarithms just got shuffled around. One has the kink $\vec{N} = (0, 1, 0)$ becoming massless at this location. Now similar to (5.12), we obtain

$$m_{\text{BPS}} = -\frac{3}{2\pi} \left(e^{2\pi i/3} - 1 \right) \Lambda + i m_1. \quad (5.14)$$

This precisely matches the second of the kinks predicted by Eq. (3.4).

Now how about the third kink? Since we know that the right-hand side of equation (2.19) is smooth in our area of attention, *and* we know that it must account for the whole

spectrum, we should be able to accommodate for the third kink with a certain choice of \vec{N} . Indeed, if one allows $\vec{N} = (0, 0, 1)$, then in the limit of small mass one has

$$m_{\text{BPS}} = -\frac{3}{2\pi} \left(e^{2\pi i/3} - 1 \right) \Lambda + i m_2, \quad (5.15)$$

which returns us the third of the kinks of Eq. (3.4).

Now, generally, the third AD point, $m_0^{\text{AD}} = -1$, is fenced from our area by branch cuts. What it in particular means, is that one cannot recover the value of m_{BPS} in that point by smoothly sliding m_0 from one of our AD points, say, $e^{i\pi/3}$ over to the third one. It does not exclude this, however, from being performed with proper accounting for the branch cuts. Even though, we can still calculate the value of (5.10) in the third AD point, arguing that whatever the branch cuts are, they are responsible for bringing $U_0(m_0^{\text{AD(III)}})$ to the resulting form. We know the answer anyway, since, it is again obtained from (5.12) by exchanging places of the logarithms, and thus numerically giving the same result. Only now this quantity, $e^{i\pi/3}$ is called differently — m_2 ,

$$U_0(-1) = -i m_2 = -i e^{i\pi/3}. \quad (5.16)$$

Since we did not follow any contour to connect this result to the Eqs. (5.12) and (5.13), we further solidify Eq. (5.16) with the following remark. In this latter equation (5.16), had it been not right, we could only be off by a branch of a logarithm of (5.10). One can fix this branch, by approaching the third AD point from the quasiclassical area, $m_0 \simeq \sigma_0 = -\infty$, and argue that the result (5.16) is precisely what one would find.

Independently of this, we notice that Eq. (5.16) *indeed is* responsible for rendering the kink (5.15) massless at $m_0^{\text{AD(III)}}$. We therefore have ascertained the strong coupling spectrum of CP(2), which consists of three kinks

$$\vec{N} = \begin{pmatrix} 1, & 0, & 0 \\ 0, & 1, & 0 \\ 0, & 0, & 1 \end{pmatrix} \quad \text{and} \quad (5.17)$$

We immediately come to the following conclusion. The first two states are part of the BPS tower of the weak-coupling region

$$\vec{N} = (-n + 1, n, 0), \quad (5.18)$$

with, correspondingly, $n = 0$ and $n = 1$. This corresponds quasiclassically to the set of states (2.21). The extra unity present in Eq. (5.18) can be explained similarly to the one in Eq. (5.5). Note that this unity could have equally well been placed into the second position of (5.18), and yet the expression would constitute the same tower.

There is no way, however, that the third state in Eq. (5.17) can be found from Eq. (2.21). The third state is an entity that makes the CP(2) model qualitatively different from CP(1), as it must be part of *another tower* of BPS states,

$$\vec{N} = (-n, n, 1). \quad (5.19)$$

This sequence of states is completely new and *invisible* in quasiclassics! More exactly, quasiclassically, the two towers blend together, as the difference between n and $n - 1$ is negligible at high excitation numbers. Furthermore, the contribution of the unity at the third position on the right-hand side of Eq. (5.19) is similarly inferior to both terms in Eq. (5.7),

$$m_{\text{BPS}} \simeq \frac{3}{2\pi} \Delta m \cdot \ln \frac{|\Delta m|}{\Lambda} + i n \cdot (m_1 - m_0) + i m_2, \quad (5.20)$$

and so is not seen quasiclassically either. The occurrence of the extra tower and the extra unity in (5.19) is a quantum phenomenon, and is the result of the fact that (any) BPS spectrum formula must describe the whole spectrum in any smooth region of m_0 — in our case, the spectrum of states given by the mirror formula (3.4), and the region shown in Fig. 2, correspondingly.

In summary, we found in CP(2) two towers of BPS states,

$$\begin{aligned} \vec{N}_{(1)} &= (-n_{(1)} + 1, n_{(1)}, 0), & n_{(1)} &\in \mathcal{Z}, \\ \vec{N}_{(2)} &= (-n_{(2)}, n_{(2)}, 1), & n_{(2)} &\in \mathcal{Z}. \end{aligned} \quad (5.21)$$

These towers merge with each other at large n , and thus are not distinguishable in the quasiclassical limit. In the strong coupling region, we find three states

$$\vec{N} = \begin{aligned} &(1, 0, 0), \\ &(0, 1, 0) \quad \text{and} \\ &(0, 0, 1), \end{aligned} \quad (5.22)$$

which form a subset of the above BPS towers: $N_{(1)}$ with $n_{(1)} = 0$ and $n_{(1)} = 1$, and $N_{(2)}$ with $n_{(2)} = 0$, correspondingly.

5.5 Spectrum in CP($N - 1$)

The crucial role which was played by equation (2.19) in the above discussion is a reflection of similarity of Eq. (2.20) and Eq. (3.4). Indeed, the structure of the latter two equations is identical — both formulas possess a factor of $e^{2\pi i/N} - 1$. In Eq. (2.20) this quantity multiplies a figure bracket which in the small m_0 limit turns into Λ and in this way matches its counterpart in Eq. (3.4). The outcome of this is that, even if the branches of the general

expression Eq. (2.14) were fixed by some method, Eqs. (2.19) and (2.20) would still play a more prominent role than the former. One other confirmation of this will be given further, when we discuss the curves of the marginal stability in Section 6.

Our discussion of the $CP(N-1)$ theory will be in vein with generalization of our previous treatment of $CP(2)$. We start with two AD points within our reference area, see Fig. 2. Choose $m_0^{\text{AD(I)}} = e^{i\pi/N}$ first. In order to determine which kink becomes massless at that point, one needs the value of $U_0(m_0^{\text{AD(I)}})$.

We find

$$U_0(m_0^{\text{AD(I)}}) = -i m_0 = -i e^{i\pi/N}. \quad (5.23)$$

This equality can either be obtained by attentively looking at the logarithms of $U_0(m_0)$ as a function, without having to calculate anything, or by actual explicit summing of all the terms in $U_0(m_0^{\text{AD(I)}})$. We instantly find from Eq. (5.23) that at $m_0^{\text{AD(I)}} = e^{i\pi/N}$ it is the kink

$$\vec{N} = (1, 0, \dots, 0) \quad (5.24)$$

that becomes massless. Tending the expression (2.20) to the limit of small m_0 , we see that this kink has the mass

$$m_{\text{BPS}} = -\frac{1}{2\pi} \left(e^{2\pi i/N} - 1 \right) \Lambda + i m_0 \quad (5.25)$$

near the origin. This obviously is one of the states of the spectrum (3.4) seen in the mirror representation.

The point $m_0^{\text{AD(I)}}$ can be smoothly connected with $m_0^{\text{AD(II)}} = e^{-i\pi/N}$, see Fig. 4. It can be shown that none of the arguments of the logarithms in the function $U_0(m_0)$ passes through a branch cut, which is what we mean by smooth. To calculate $U_0(m_0^{\text{AD(II)}})$ one, however, can use Eq. (5.23). The value of function $U_0(m_0)$ numerically is the same in all AD points, while at the point $m_0 = e^{-i\pi/N}$ we just endow it with a different name,

$$U_0(m_0^{\text{AD(II)}}) = -i m_1 = -i e^{i\pi/N}. \quad (5.26)$$

This means that the kink

$$\vec{N} = (0, 1, \dots, 0) \quad (5.27)$$

becomes massless at $m_0^{\text{AD(II)}}$. In the limit of small m_0 , the mass of this kink takes the form

$$m_{\text{BPS}} = -\frac{1}{2\pi} \left(e^{2\pi i/N} - 1 \right) \Lambda + i m_1, \quad (5.28)$$

which, again, corresponds to one of the states described by the mirror formula (3.4). The above two kinks are part of the same tower of BPS states

$$\vec{N} = (-n + 1, n, \dots, 0), \quad (5.29)$$

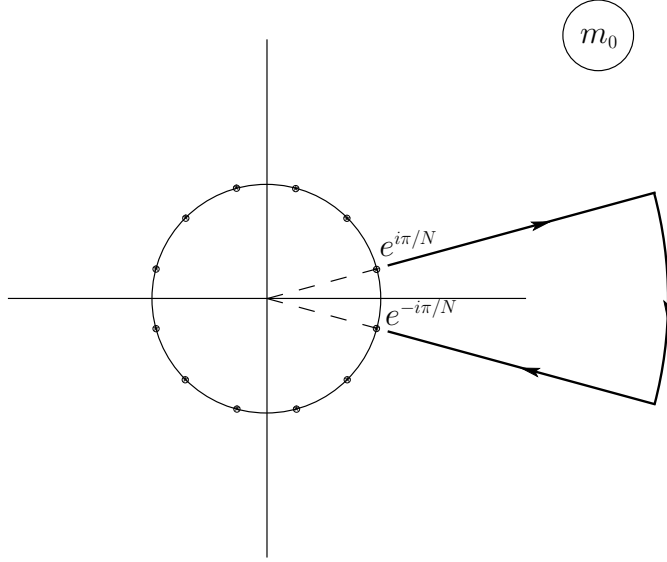


Figure 4: The contour connecting two AD points $m_0^{\text{AD(I)}} = e^{i\pi/N}$ and $m_0^{\text{AD(II)}} = e^{-i\pi/N}$ in $\text{CP}(N - 1)$ theory.

which exists in the weak coupling region. Equations (5.24) and (5.27) represent the states with $n = 0$ and $n = 1$, respectively.

All other AD points, although maybe disconnected from our region of interest by branch cuts, can still be easily dealt with, since we know the value of $U_0(m_0)$ for any AD point,

$$U_0(m_0^{\text{AD}}) = -i e^{i\pi/N}. \quad (5.30)$$

For the extra $N - 2$ AD points, one has, therefore,

$$U_0(m_0^{\text{AD}}) = -i m_k, \quad \text{with } k = 2, \dots, N - 1. \quad (5.31)$$

It does not matter which AD point produces what mass on the right-hand side, the only important thing is that all other masses m_k with $k \geq 2$ pop up on the right-hand side. As it can be easily seen, in terms of the vector \vec{N} , this corresponds to the kinks becoming massless at the respective AD points. The index k effectively shifts the unity in Eqs. (5.24) and (5.27) further to the right. The full set of the states which become massless then looks as,

$$\vec{N} = \begin{pmatrix} 1, & 0, & 0, & \dots, & 0 \\ 0, & 1, & 0, & \dots, & 0 \\ 0, & 0, & 1, & \dots, & 0 \\ \cdot & \cdot & \cdot & \cdot & \cdot \\ 0, & 0, & 0, & \dots, & 1 \end{pmatrix}. \quad (5.32)$$

Now in the limit of small masses m_0 we precisely obtain the full spectrum (3.4) predicted by the mirror representation,

$$m_{\text{BPS}} = -\frac{1}{2\pi} \left(e^{2\pi i/N} - 1 \right) \Lambda + i m_k, \quad k = 0, \dots, N-1. \quad (5.33)$$

In the weak-coupling spectrum, the states (5.32) belong to towers. The first two states are part of one and the same tower (5.29), while of the rest of the states each belongs to its own one. This agrees with a generic expectation to have $N-1$ towers, according to the breaking of the global $SU(N)$ by the masses, $SU(N) \rightarrow U(1)^{N-1}$. The spectrum (5.21) of the $CP(2)$ theory is then obviously extended for an arbitrary N ,

$$\begin{aligned} \vec{N}_{(1)} &= (-n_{(1)} + 1, \quad n_{(1)}, \quad 0, \quad 0, \quad \dots, \quad 0), \\ \vec{N}_{(2)} &= (\quad -n_{(2)}, \quad n_{(2)}, \quad 1, \quad 0, \quad \dots, \quad 0), \\ \vec{N}_{(3)} &= (\quad -n_{(3)}, \quad n_{(3)}, \quad 0, \quad 1, \quad \dots, \quad 0), \\ &\cdot \quad \cdot \\ \vec{N}_{(N-1)} &= (\quad -n_{(N-1)}, \quad n_{(N-1)}, \quad 0, \quad 0, \quad \dots, \quad 1), \end{aligned} \quad (5.34)$$

with all $n_{(k)}$ integer numbers. Obviously, in the quasiclassical limit, these towers reproduce the asymptotics (2.21), and therefore satisfy all three criteria which we listed in the end of Section 5.1. Note, that the total number of states in the physical weak-coupling spectrum is $(N-1)\mathcal{Z}$, much less than the total multiplicity \mathcal{Z}^N allowed by (2.19).

Equations (5.34) and (5.32) are our main results for the spectrum of the $CP(N-1)$ model in the weak- and strong-coupling regimes, respectively. They exhibit a drastic difference with what was thought of the spectrum of $CP(N-1)$ earlier [5], when it was argued that only one tower of the BPS states existed (for a given pair of vacua, of course). We stress that the emergence of the extra $N-2$ towers is a pure quantum effect which could not be anticipated in the quasiclassical theory. All of $N-1$ towers of states blend and become degenerate in the quasiclassical limit, making it hard to resolve them apart.

6 Curves of Marginal Stability

The fact that there are $N-1$ towers of BPS states means that there should be $N-1$ curves on which those towers collapse. Looking at Eq. (5.34) one can tell that the first of them is special, just by its appearance — the unity stands in one row with $n_{(1)}$ (it is a mere matter of convention whether to write this unity in the first or in the second position). We will find that this tower is also special for an objective reason — namely, its decay curve will necessarily pass through the AD point, while those of the other towers will not. For the

same token, it will also be the *innermost* curve. That is, inside this decay curve, only strong coupling states (5.32) exist.

We provide an important technical remark on the graphical illustrations in the following discussion. We will choose to draw curves of marginal stability in the plane of m_0^N rather than in that of m_0 . Due to 2π -periodicity in θ -angle, a curve sketched in the m_0 plane repeats itself N times in each of $2\pi/N$ sectors of the argument of m_0 . This way, drawing a curve in the m_0^N plane is as informative. We call for attention however, that when drawing multiple curves, we will have to do special rescaling in the m_0^N plane, for the sake of fitting multiple figures in one plot.

Having the spectrum of the theory at hand, it does not cost an effort to write the equations for the curves of marginal stability. Each such equation needs to rephrase the condition that one of the towers (5.34) completely decays. Let us write explicitly the expression for the mass of a BPS state as per the spectrum (5.34),

$$m_{\text{BPS}} = U_0(m_0) + i n_{(k)} \cdot (m_1 - m_0) + i m_k, \quad k = 1, \dots, N - 1. \quad (6.1)$$

Here for sake of convenience we redefined the U(1) charge $n_{(1)}$ in (5.34) with

$$n_{(1)} \rightarrow n_{(1)} + 1.$$

In terms of the expression for the mass, the “tower” is given by the term

$$i n_{(k)} \cdot (m_1 - m_0).$$

For the tower to decay, the remainder in the right-hand side of Eq. (6.1) must be in phase with the latter term, or

$$\text{Re} \frac{U_0(m_0) + i m_k}{m_1 - m_0} = 0. \quad (6.2)$$

This is the CMS equation. We obtain $N - 1$ curves here by letting k run from 1 to $N - 1$.

Now, we can make a few assertions on CMS before starting drawing them:

- The curves (6.2) either do not intersect or they completely overlap;
- The *primary* curve corresponding to $k = 1$ (and only this curve) passes through the AD point.

The first assertion is seen from Eq. (6.2) directly. If the curves with $k = p$ and $k = q$ happen to intersect somewhere, then

$$\frac{m_p - m_q}{m_1 - m_0} \in \mathcal{R} \quad (6.3)$$

at that place. But this ratio does not depend on the absolute value of m_0 , nor on its phase, so it will remain real along both of the curves, which for this reason will have to completely match. We will find that this does happen all along.

The second assertion, although obvious as well, deserves more attention. To see that the curve $k = 1$ passes through the AD point, we rewrite Eq. (6.2) as

$$\operatorname{Re} \frac{U_0(m_0) + i m_0}{m_1 - m_0} = 0, \quad (6.4)$$

where the substitution $m_1 \rightarrow m_0$ in the numerator obviously does not change the condition (in fact, Eq. (6.4) is exactly what we would have obtained from the spectrum (5.34) if we had not done the shift of $n_{(1)}$ above). But we calculated the value of $U_0(m_0)$ at the AD point $m_0^{\text{AD}(1)}$ in Eq. (5.23), which shows that the CMS condition is trivially met there. Then the curve has to pass through all AD points.

In the m_0^N plane there is just one such point, and, since σ_p vanishes in it, we can expand the above condition in σ_0/m_0 in its neighborhood. We have,

$$\operatorname{Re} \sum_{r>0} \frac{\alpha^{rN+1}}{rN+1} = 0, \quad \alpha = \frac{\sigma_0}{m_0}. \quad (6.5)$$

This function, up to a constant, is actually known as the so-called Hurwitz–Lerch transcendent, and is a special case of the hypergeometric function. For our purposes, however, we only need the leading order term of it,

$$\operatorname{Re} \alpha^{N+1} = 0, \quad \text{for } \alpha \ll 1. \quad (6.6)$$

Solving this equation gives us the *angle* at which the $k = 1$ curve passes through the AD point,

$$\phi = \begin{cases} + \frac{N+2}{N+1} \cdot \frac{\pi}{2}, \\ 0, & \text{(for CP(1) only)} \\ - \frac{N+2}{N+1} \cdot \frac{\pi}{2}, \end{cases} \quad (6.7)$$

where, as customary, we measure the angle from the real positive direction counter-clockwise. Equation (6.7) tells us that for $N > 2$ there are two opposite angles, and the decay curve has a *cusp* at the Argyres–Douglas point, see Fig. 5. As N becomes larger, the opening angle of the cusp increases, and ultimately, when N is taken infinitely large the curve becomes smooth.

CP(1) theory is special, as its curve has three angles $+120^\circ$, -120° and 0° instead of two. The third angle corresponds to the extra flat part $[-1, 0]$ of the curve sticking out of the AD point, see Fig. 6. Otherwise, the CP(1) case is the simplest, and so we start the illustrative part of our discussion with this theory.

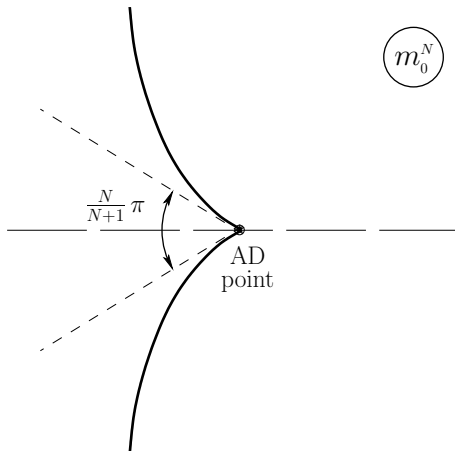


Figure 5: The cusp of the primary decay curve at the AD point in the m_0^N plane.

6.1 The decay curve in CP(1)

There is just one curve of marginal stability in CP(1) and it is the primary one. It represents a sharp boundary between the areas of weak and strong coupling spectra. This curve and its features have been discussed in the literature [6, 9], so we just merely reproduce it with Eq. (6.2). Figure 6 shows the curve in the plane of m_0^2 . The whole graph is presented in units of Λ^2 . We re-state the known facts that the curve has a cusp at the AD point, where also an extra part $[-1, 0]$ of the curve connects. All three lines meet at the AD point at an angle 120° with respect to each other. The real interval $[-1, 0]$ is the analytical solution to the CMS condition. There is nothing like that for any other CP($N - 1$) theory, all other curves are just curves.

6.2 CMS in CP(2) theory

The CP(2) theory features two curves — one primary and one secondary. The primary curve, as we established, has a cusp at the AD point with the opening angle 135° , see Fig. 7.

The second curve is a circle-like loop with a radius of approximately $361 \Lambda^3$ (as we will see, it *is* a circle to a very good accuracy). This is a very large circle, compared to the primary curve which is of the size Λ^3 . In order to plot them both on the same graph, we rescale the *radial* direction of m_0^N by taking the N -th root from its absolute value, while leaving the phase of m_0^N as is,

$$|m_c| \equiv |m_0^N|^{1/N}, \quad \text{Arg } m_c = \text{Arg } m_0^N. \quad (6.8)$$

The subscript c stands for compressed. Figure 8 shows the two curves in the rescaled m_0^3

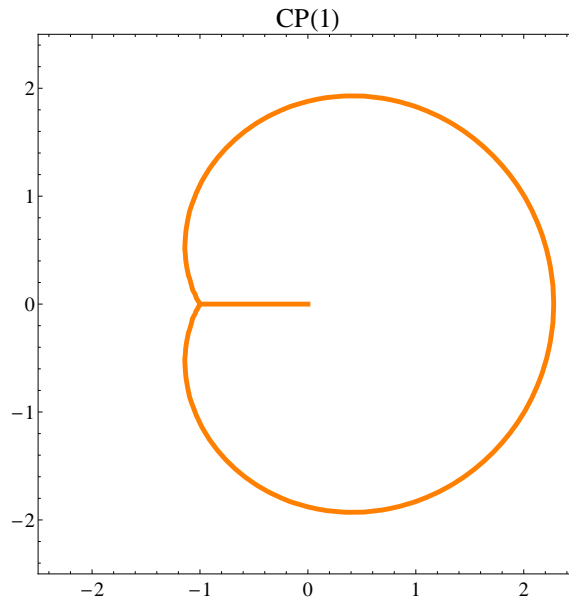


Figure 6: The curve of marginal stability in CP(1) theory (m_0^2 plane), Ref. [6].

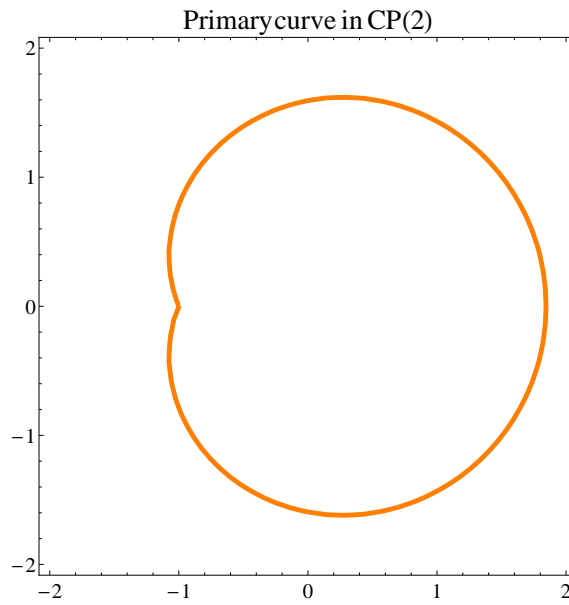


Figure 7: The primary decay curve in the CP(2) theory (m_0^3 plane).

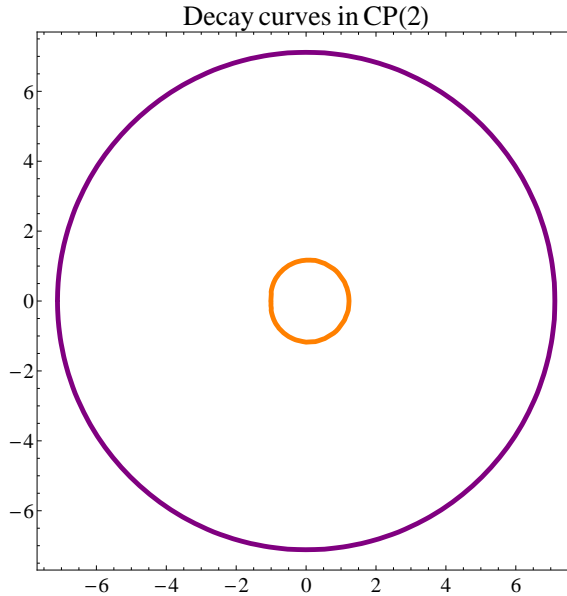


Figure 8: Both decay curves in the CP(2) theory (compressed m_c plane, see text).

plane. This compression will appear useful for the large N case. Such a transformation, certainly, distorts the cusp making it less expressed. But, Figure 7 assures us that it is there, and Figure 5 tells us that it is there for all CP($N - 1$).

The radius of the external curve, $361 \Lambda^3$ is found to be rather large. However, in the compressed m_c plane (Fig. 8), and, equivalently, in the m_0 plane, the curve has the size approximately 7.12Λ . We will find later, that the maximal radius of all curves (in the large N limit) is $e^2 \Lambda$, which amounts to 7.39Λ . Thus, already the secondary curve of CP(2) nearly saturates the maximum size.

6.3 Larger- N theories

For the CP(3) theory, the curves are shown in Fig. 9. Again, we plot the curves in the plane where m_0^N was radially compressed to m_c . The two outer curves in CP(3) overlap, as a consequence of Eq. (6.3),

$$m_2 - m_3 = m_1 - m_0. \quad (6.9)$$

The cusp in the primary curve is still present, although is flattened in Fig. 9 due to compression.

For CP(4) the curves are shown in Fig. 10. The overlapping curves are shown with portioned lines. The radius of the outer most curve is 7.33Λ , which is very close to the upper limit! Figures 11 and 12, as an illustration, show the curves for the CP(6) and CP(9).

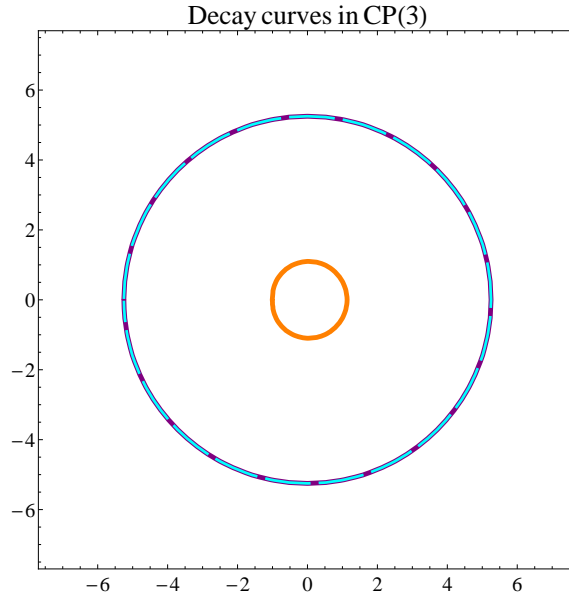


Figure 9: Three decay curves in the CP(3) theory (compressed m_c plane, see Eq. (6.8)).

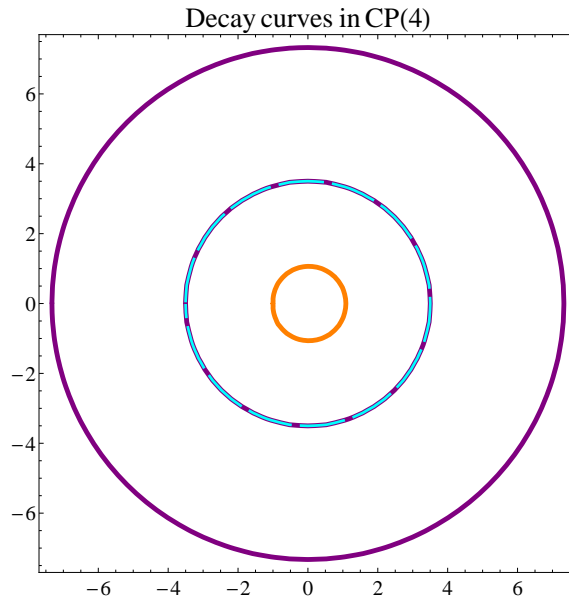


Figure 10: The decay curves in the CP(4) theory (compressed m_c plane, see Eq. (6.8)). External radius is 7.33Λ .

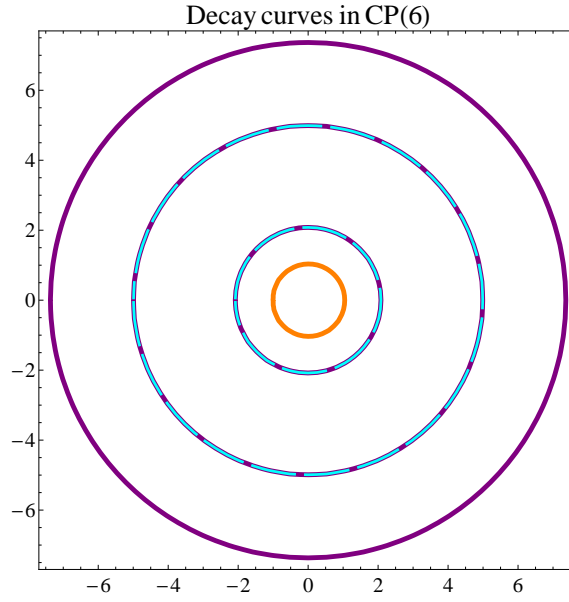


Figure 11: The decay curves in the CP(6) theory (compressed m_c plane). Outer radius is 7.37Λ .

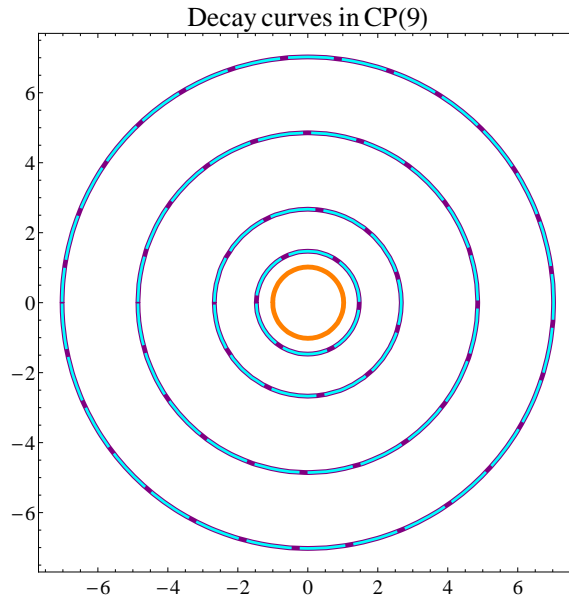


Figure 12: The curves in CP(9) theory (compressed m_c plane). Outer radius is 7.02Λ .

Let us briefly review the main features of these plots. We observe that all decay curves look as nearly perfect circles. We do not set the goal here to rigorously prove that they are, but we are able to show that the secondary curves for a few first theories are circles to a good accuracy and have no reason to believe that this is not so for larger N . More detailed analysis of their shape lies outside the scope of this paper.

We know that the primary curves are not circular because of the cusp, and if in our figures they look round, this is just an illusion caused by the compression. For example, for CP(9) with N as large as 10, the cusp opening angle would be 164° , which although close to 180° , would still be quite noticeable. It is true, however, that at larger N even the primary curves turn into circles (that is, in any plane). We will discuss this in the next subsection.

However, the secondary curves are circular even for small N . Using the $(\Lambda/m_0)^N$ expansion of the CMS condition (6.2) it is possible to prove the following statement. If it is known, that a particular curve passes at a large distance from the origin at least at one point, then such a curve must be a circle as perfect as $(\Lambda/m_0)^N$. For example, in CP(2), Fig. 8, the outer curve is a circle with the accuracy about $1/360$. This remark allows us to see that the secondary curves are round for a few starting CP($N - 1$) theories, just by looking at the location where the curves cross the real axis. For the primary curves this statement obviously does not apply since they pass through the AD point at a unit distance from the origin.

For larger N , the $k = 2$ curves come closer and closer to the primary one, and one might suspect that they start losing their shape. For example, the radius of the $k = 2$ curve in CP(14) theory is only ~ 14 in units of Λ^{15} . A deviation from a circular figure at the level of $1/14$ would be quite noticeable. However, a different effect takes over, which helps the decay curves stay “fit”.

6.4 Curves in the large- N limit

We now consider the question of the form of the decay curves in the limit of large N . It turns out that the analysis greatly simplifies. All the curves turn into circles of a certain radius.

As usual, the primary curves are a separate topic. Consider the curve in the neighborhood of the AD point, where it is described by Eq. (6.5),

$$\operatorname{Re} \sum_{r>0} \frac{\alpha^{rN+1}}{rN+1} = 0, \quad (6.10)$$

and discard the unity in the denominator. The sum then reassembles into a logarithm,

$$\operatorname{Re} \frac{\sigma_0}{m_0} \log \left(1 - \frac{\sigma_0^N}{m_0^N} \right) = 0, \quad (6.11)$$

where we have replaced α with its definition. As N goes to infinity, the vacuum σ_0 approaches the value m_0 , and we can replace the ratio σ_0/m_0 in front of the logarithm with unity. The logarithm itself can be transformed into

$$\text{Re} \log \left(- \frac{\Lambda^N}{m_0^N} \right) = 0. \quad (6.12)$$

This equation is trivially solved if $(m_0/\Lambda)^N$ is a pure phase. The curve then has to be a circle everywhere, not only in the region of validity of expansion (6.10). We thus have shown that at large N all primary curves tend to a circle of unit radius (in units of Λ^N).

A similar idea, but in a different realization is used to reveal the shapes of the secondary curves. In the region of space where $|\sigma_0| > |m_0|$ (in particular, at large positive m_0) one can expand the CMS condition in $1/\alpha$. This gives,

$$- \text{Re} \sum_{r \geq 0} \frac{\alpha^{-(rN-1)}}{rN-1} = \frac{2\pi \cos \frac{2k-1}{N} \pi}{2 \sin \frac{\pi}{N}}, \quad (6.13)$$

where k , again, is the number of the curve. At large N we can again drop the unity in the denominator on the left hand side, which turns the sum into a logarithm. Also we expand the sine in the right hand side to the leading order in $1/N$. We have

$$1 - \ln |\sigma_0 / \Lambda| = \cos \frac{2k-1}{N} \pi. \quad (6.14)$$

Replacing σ_0 with m_0 with an exponential accuracy, we arrive at the formula,

$$|m_0| = e^{1 - \cos \frac{2k-1}{N} \pi}, \quad k = 1, \dots, N-1, \quad (6.15)$$

in units of Λ . Even though this formula has been derived in the assumption of large N , it *qualitatively* gives a reasonable answer even for N as low as three!

The qualitative features, which are obeyed in all $\text{CP}(N-1)$ theories at large N are as follows. The curves come in overlapping pairs, as given by the cosine in Eq. (6.15). The *minimum* radius of the CMS is one, and is saturated by the primary curve — this fact we already know. The *smallest secondary* curves correspond to $k = 2$ and $k = N-1$. Their size depends on N . Finally, the *maximum* size is

$$m_0^{\max} = e^2, \quad (6.16)$$

measured in units of Λ , and is reached by the $k = \frac{N+1}{2}$ or the $k = \frac{N+1 \pm 1}{2}$ curves, depending on parity of N . For odd N , the largest curve does not have an overlapping party.

Interestingly enough, although these qualitative results were inferred from the large- N formula (6.15), they are still valid for small N theories! In particular, e^2 seems to be the

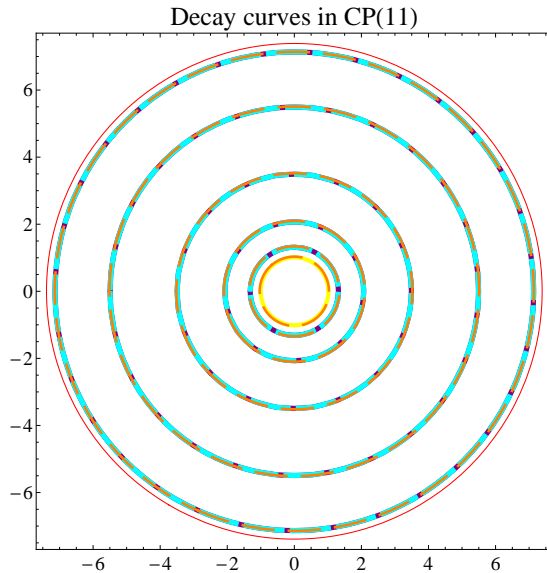


Figure 13: The curves in the CP(11) theory (compressed m_c plane).

absolute limit for the size of all of the curves (the deviation is that this limit is not attained at small N , but some curves do come very close as we saw above). Also, the pairing of overlapping curves described by the cosine appears to be correct for any N .

We illustrate the large N limit formula (6.15) in Fig. 13. The external thin circle envelopes the overall $|m_0| = e^2$ size of the figure. The circles of radii determined by Eq. (6.15) are shown with thin dashed lines, which perfectly overlay the numerical curves. In fact, the latter formula has a good agreement with CMS curves already for $N = 8$, while, as we mentioned, in overall it shows the right tendency already for N as low as three.

As we increase N , the decay curves fill in the whole interval

$$|m_0| \in 1 \dots e^2. \quad (6.17)$$

Formula (6.15) predicts how the curves lay into this interval. As a concluding illustration, Fig. 14 shows the curves of the CP(100) theory.

7 Prospects for the Spectrum in Quasi-Classics

We have used strong coupling techniques, such as the mirror symmetry, in order to establish the form of the BPS spectrum,

$$m_{\text{BPS}} = U_0(m_0) + i n_{(k)} \cdot (m_1 - m_0) + i m_k, \quad k = 1, \dots, N - 1. \quad (7.1)$$

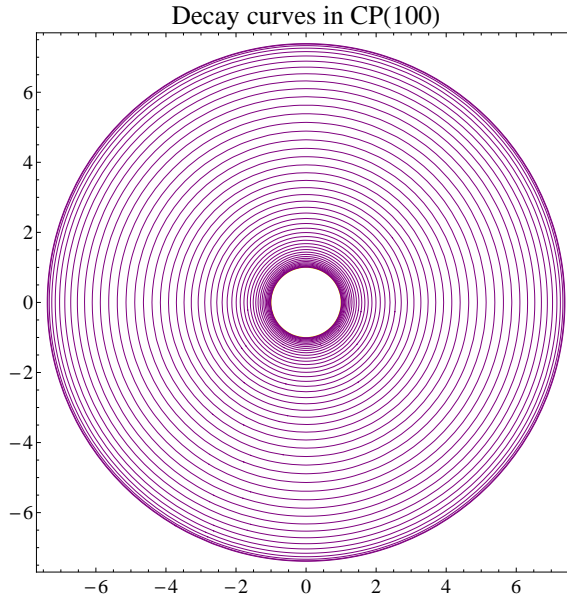


Figure 14: The curves in the CP(100) theory (compressed m_c plane).

At weak coupling, it must also be possible to see the features of this result, via semi-classical methods. At large m , function $U_0(m_0)$ gives the canonical logarithmic contribution as shown in Eq. (5.7), while the mass difference $m_1 - m_0$ constructs the towers. These two contributions are expected. A very non-trivial prediction of Eq. (7.1) is the last term, which distinguishes the different towers. If one re-writes all relevant equations in terms of the mass differences, then

$$m_k = \frac{1}{N} \sum_j (m_k - m_j), \quad (7.2)$$

since the average mass is zero in our case. This shows in fact that the last term in Eq. (7.1) represents a fractional U(1) charge.

The phenomenon of the occurrence of a fractional charge is well-known [22, 6, 23, 24], and is due to the presence of fermions. In particular, for CP(1) one has a half-unit contribution to the central charge [6]. We observe this one half by re-writing the last term of Eq. (7.1) in terms of the mass difference

$$i m_1 = -i m_0 = \frac{1}{2} i \Delta m, \quad (7.3)$$

which acts as a half-integer addition to $n_{(1)}$. Therefore in the CP(1) model there is an agreement between our spectrum and the known quasi-classical results. Recovery of the weak-coupling spectrum in a general CP($N - 1$) theory via semi-classical methods is an

important and non-trivial problem deserving a separate study. We plan to address this topic elsewhere.

8 Conclusion

We demonstrated that the weak-coupling spectrum of the $\text{CP}(N-1)$ theory with twisted \mathcal{Z}_N masses is considerably richer than was thought before. In particular, there are $N-1$ infinite towers of the BPS states. Our analysis relied on three important facts known about $\text{CP}(N-1)$: the strong coupling spectrum only includes N states; these states become massless at the Argyres–Douglas points; quasiclassical spectrum contains a tower of states with integer $U(1)$ charges. The knowledge of the exact superpotential is not sufficient as it is ambiguous. However, if one fixes this ambiguity at least in some region of the parameter space, then the superpotential must still describe the states in the strong coupling domain. It is possible to trace these states all the way from the weak-coupling region through the AD points and into the strong-coupling domain, where their masses can be fixed by comparing with the mirror representation. We emphasize that we observe $N-1$ towers instead of just one, which is naturally explained by the fact that the global $\text{SU}(N)$ symmetry is broken down to $N-1$ copies of $U(1)$, and the central charges of the model include terms proportional to $N-1$ Noether charges. However, only one of these towers is seen quasiclassically. Furthermore, these $N-1$ towers blend together in the quasiclassical limit, making it hard to anticipate their existence from the semiclassical analysis alone.

Having obtained the spectrum, it is easy to construct the curves of the marginal stability. We find $N-1$ such curves, one per each BPS tower. One of the curves, which we refer to as primary, is special as it passes through the AD point, with necessity. Inside this curve, only N stable states of the strong coupling spectrum survive. We also considered the large- N limit and argued that all curves tend to a circular shape, with the radius lying in between 1 and e^2 , in units of Λ .

We note that we only analyzed the decay curves of elementary states. In principle, nonelementary kinks have their own series of curves [25]. Also, the theory must have the fermion-soliton bound states [26], for which there will exist CMS as well.

As was shown in [5], the BPS spectrum of dyons (at the singular point on the Coulomb branch in which N quarks become massless) of $\mathcal{N} = 2$ four-dimensional supersymmetric QCD with the $U(N)$ gauge group and $N_f = N$ quark flavors, identically coincides with the BPS spectrum in the two-dimensional $\text{CP}(N-1)$ model. The reason for this coincidence was revealed in [1, 2]. The confined 't Hooft–Polyakov monopoles of the four-dimensional theory are represented by junctions of two different non-Abelian strings. The effective theory on the world sheet of the non-Abelian string is the two-dimensional $\text{CP}(N-1)$ model [3, 4, 1, 2].

Confined monopoles of the bulk theory are seen in the world-sheet theory as kinks of the $CP(N - 1)$ model. This ensures the coincidence of the BPS spectra in both theories, see [1, 2] for more details.

The above coincidence implies that we can use the results for BPS spectrum of the $CP(N - 1)$ model obtained in this paper to construct the physical spectrum of the BPS dyons in $\mathcal{N} = 2$ supersymmetric QCD in the particular vacuum in which N quarks become massless. More specifically, the masses of the BPS states in four dimensions are given by the periods of the Seiberg–Witten differential, and have exactly the same form as the central charge of the sigma model (2.13) written in terms of the Veneziano–Yankielowicz superpotential. The masses of dyons are determined by the contours that encircle the branch points of the Seiberg–Witten curve. The spectrum that we derived in the sigma model gives the prescription on how to build contours that correspond to stable BPS states. In particular, our result (5.34) for the weak-coupling spectrum of the $CP(N - 1)$ model suggests that the dyon electric charges in the bulk theory, besides the towers built on the roots of the gauge group, also contain contributions determined by its weights, cf. [27]. The question of the correspondence between the spectra of the BPS states and the decay curves of dyons of the two theories calls for a special investigation.

Acknowledgments

The work of MS was supported in part by DOE grant DE-FG02-94ER408. The work of PAB is supported by the DOE grant DE-FG02-94ER40823. The work of AY was supported by FTPI, University of Minnesota, by RFBR Grant No. 09-02-00457a and by Russian State Grant for Scientific Schools RSGSS-65751.2010.2.

References

- [1] M. Shifman and A. Yung, Phys. Rev. D **70**, 045004 (2004) [hep-th/0403149].
- [2] A. Hanany and D. Tong, JHEP **0404**, 066 (2004) [hep-th/0403158].
- [3] A. Hanany and D. Tong, JHEP **0307**, 037 (2003) [hep-th/0306150].
- [4] R. Auzzi, S. Bolognesi, J. Evslin, K. Konishi and A. Yung, Nucl. Phys. B **673**, 187 (2003) [hep-th/0307287].
- [5] N. Dorey, JHEP **9811**, 005 (1998) [hep-th/9806056].
- [6] M. Shifman, A. Vainshtein, R. Zwicky, J. Phys. A **A39**, 13005-13024 (2006). [hep-th/0602004].

- [7] A. Hanany and K. Hori, Nucl. Phys. B **513**, 119 (1998) [arXiv:hep-th/9707192].
- [8] G. Veneziano and S. Yankielowicz, Phys. Lett. B **113**, 231 (1982).
- [9] S. Ölmöz and M. Shifman, J. Phys. A **40**, 11151 (2007) [arXiv:hep-th/0703149].
- [10] P. A. Bolokhov, M. Shifman, A. Yung, Phys. Rev. **D82**, 025011 (2010). [arXiv:1001.1757 [hep-th]].
- [11] M. Shifman, A. Yung, Phys. Rev. **D81**, 085009 (2010). [arXiv:1002.0322 [hep-th]].
- [12] K. Hori and C. Vafa, *Mirror symmetry*, arXiv:hep-th/0002222.
- [13] P. C. Argyres and M. R. Douglas, Nucl. Phys. **B448**, 93 (1995) [arXiv:hep-th/9505062].
- [14] E. Witten, Nucl. Phys. B **403**, 159 (1993) [hep-th/9301042].
- [15] L. Alvarez-Gaumé and D. Z. Freedman, Commun. Math. Phys. **91**, 87 (1983); S. J. Gates, Nucl. Phys. B **238**, 349 (1984); S. J. Gates, C. M. Hull and M. Roček, Nucl. Phys. B **248**, 157 (1984).
- [16] A. D’Adda, A. C. Davis, P. DiVecchia and P. Salamonsen, Nucl. Phys. **B222** 45 (1983).
- [17] S. Cecotti and C. Vafa, Comm. Math. Phys. **158** 569 (1993) [hep-th/9211097].
- [18] E. Frenkel and A. Losev, Commun. Math. Phys. **269**, 39 (2006) [arXiv:hep-th/0505131].
- [19] N. Seiberg and E. Witten, Nucl. Phys. **B426**, 19 (1994), (E) **B430**, 485 (1994) [hep-th/9407087].
- [20] A. Bilal, F. Ferrari, Nucl. Phys. **B480**, 589-622 (1996). [hep-th/9605101].
- [21] A. Bilal, F. Ferrari, Nucl. Phys. **B516**, 175-228 (1998). [hep-th/9706145].
- [22] R. Jackiw, C. Rebbi, Phys. Rev. **D13**, 3398-3409 (1976).
- [23] M. Shifman, Lect. Notes Phys. **659**, 237-284 (2005).
- [24] M. Shifman, A. Yung, Rev. Mod. Phys. **79**, 1139 (2007). [hep-th/0703267].
- [25] S. Lee, P. Yi, JHEP **1003** (2010) 055 [arXiv:0911.4726 [hep-th]].
- [26] N. Dorey, T. J. Hollowood, D. Tong, JHEP **9905**, 006 (1999). [hep-th/9902134].
- [27] C. Fraser, T. Hollowood, Nucl. Phys. **B490** (1997) 217 [hep-th/9610142].